This full text paper was peer reviewed at the direction of IEEE Communications Society subject matter experts for publication in the IEEE Globecom 2010 proceedings.

Characterization and Evaluation of In-Vehicle Power Line Channels

Ana Belén Vallejo-Mora[1], Juan José Sánchez-Martínez, Francisco Javier Cañete[2], José Antonio Cortés, Luis Díez
Departamento de Ingeniería de Comunicaciones
E.T.S.I. de Telecomunicación, University of Málaga, Spain
Email: [1]abvm@ic.uma.es, [2]francis@ic.uma.es

***Abstract*—This paper presents a statistical characterization of in-vehicle power lines, based on channel measurements carried out in a automobile. In particular, the impact of the engine speed on the characteristics of the channels is analyzed. Performance of an Orthogonal Frequency-Division Multiplexing (OFDM) system is assessed using the channel measurements.**

I. Introduction

Nowadays, in-vehicle equipment is being continuously improved in terms of safety, reliability and comfort. These sophisticated devices include passive safety systems such as airbags, and active safety systems like Electronic Stability Program (ESP), Adaptive Cruise Control (ACC) and functions related to the steering and traction. On the other hand, vehicle design increasingly includes less mechanical systems and more electronic equipment (injection, lighting systems, etc). As a result, the number of sensors and actuators has been increased, which need to be connected with each other and with a central control system. For this purpose, protocols in the automotive field that use dedicated buses as CAN (Controller Area Network), LIN (Local Interconnect Network) and Flexray have been proposed. At present, power line communication (PLC) represents a new alternative that offers numerous advantages. This technology uses the power lines inside the car as a transmission medium and allows eliminating some of the wiring harnesses actually devoted to convey data signals. This benefit is directly translated into a reduction of car production cost, vehicle weight and fuel consumption.

Besides, PLC would allow to add new features that need to incorporate electronic circuits, without any other cables. Although it has been originally conceived as a redundant network to complement existing ones, in the future, specific cables could be eliminated if PLC demonstrates the necessary reliability.

We have carried out channel response measurements on a vehicle. Three different engine states have been evaluated, with the engine turned off ('Off'), with the engine running at approximately 750 revolutions per minute ('Idle') and with the engine running at 2000 revolutions per minute ('2000 rpm'). Statistical parameters of the measurements have been obtained and analyzed. In-vehicle PLC channels are frequency selective [1],[2] due to multipath propagation phenomena caused by impedance mismatching in the wires. To face this frequency selectivity Multicarrier Modulation (MC) has been proven as a suitable technique. Some previous works [3], [4] have evaluated Orthogonal Frequency Division Multiplexing (OFDM) studying the feasibility of PLC indoor standards (HomePlug and HD-PLC) in-vehicles. On the other hand, the recently approved ITU-T G.hn recommendation for in-home networking has been a milestone to overcome the lack of an international technical standard and so that to promote the expansion of PLC technology. In [5] we have assessed the performance of OFDM systems on indoor PLC channels according to the upcoming G.hn standard and here we evaluate the performance of the new standard modulation scheme on automotive networks.

This paper is organized as follows. Firstly, the measurement setup is described in section II. Obtained results and statistical channel characterization are presented in section III and section IV, respectively. Performance analysis of MC systems over the measured channels is assessed in section V. Finally, conclusions are summarized in section VI.

II. Measurement setup

Channel and noise broad-band measurements have been carried out in a Fiat car. The transfer function measurements were accomplished in the frequency domain by means of a Vector Network Analyzer (VNA). S_{11} and S_{21} parameters, with $Z_0 = 50\ \Omega$ as reference impedance value have been measured. The selected VNA frequency range goes from 300 kHz to 100 MHz with 1601 frequency samples. A digital oscilloscope with a 8 bits data acquisition card (DAC) is employed for the noise measurements. The sampling frequency is fixed to 200 MHz and data registers of lenght up to 20 ms are captured. An High Pass Filter (HPF) is used to remove DC voltage when needed.

A. Measured links

Two criteria have been considered for choosing access points. Firstly, with respect to the location of the measurement points, we have tried to distribute them uniformly along the car. Secondly, regarding the power supply, there are two types of access points. Those directly connected to the battery (always powered) and those only powered when the engine is turned on.

Fig. 1 shows the locations for communication nodes: the battery (BAT), the cigarette lighter (CIG), the radio system (RAD), the fuse box (FUS), the right front turn signal light (FrontRTS), the left low beam headlight (FrontLBE), the

978-1-4244-5637-6/10/$26.00 ©2010 IEEE

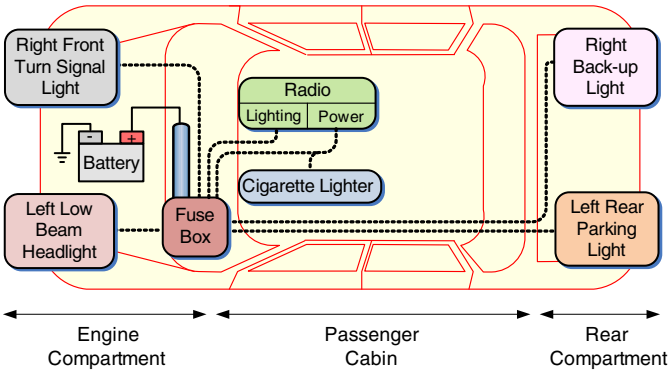

Fig. 1. Chosen access points along the car

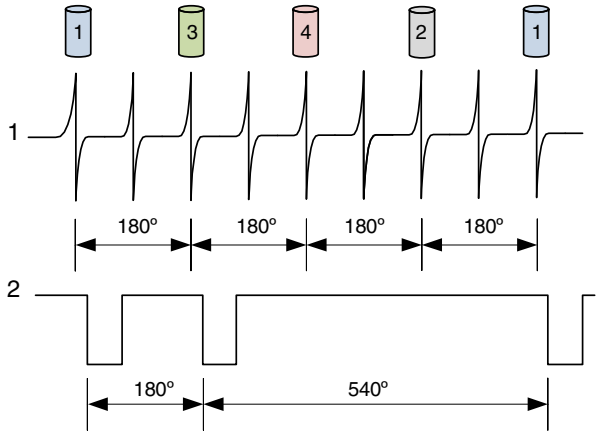

Fig. 2. Engine cycle: 1. Speed signal 2. Phase signal.

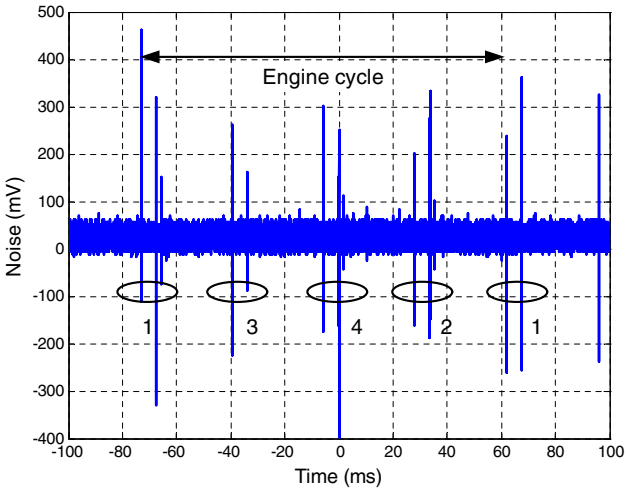

Fig. 3. Measured noise at CIG access point. Sampling frequency fixed to 20 MHz to capture the noise during 200 ms. The numbers indicate the involved cylinder.

left rear parking light (RearLPA) and right back-up light (RearRBAC).

Two access points have been utilized on the RAD, the power supply connector (RADP) and the lighting power connector (RADL). In the case of the fuse box, we have selected two fuses that protect different circuits:

- (FUSA) instrument panel lights, right rear parking light, left license plate light and left front parking light.
- (FUSB) front panel power supply, windscreen wiper motor, back-up lights and fuel injection control system.

We have measured twelve channels that join different combination of these access points. Channels responses are measured changing the engine speed. All channels pass through the battery, except the link RADP-CIG. The links connected through the battery have their transmitter and receiver access points behind different fuses in the fuse box. In the link RADP-CIG, both the radio power supply and the cigarette lighter power supply, reach the same fuse.

B. Electronic Control Unit: Speed and phase signals

The Electronic Control Unit (ECU) is a microprocessor that gets all the data on engine operating conditions from different sensors. Through these signals, the ECU controls the start of fuel injection and the injection time. There are two signals of interest: the speed signal and the phase signal. The speed signal indicates the revolutions per minute that the engine achieves at each instant, and the phase signal allows the four cylinders synchronism. Eight periods of speed signal and one period of phase signal occur during an engine cycle (see Fig. 2).

During the injection phase a spark is produced by the spark plug of each cylinder. It generates an impulsive signal of high voltage, so that four impulses occur during an engine cycle. These signals appear on the measured noise at different access points. For instance, Fig. 3 shows the measured noise at the cigarette lighter. It can be observed a noise register that includes six sparks and their replicas.

C. Engine States

Due to the increase of noise power that occurs when the engine is running, we have considered different engine states, that include:

- 'Off': The engine is turned off. Only some electronic systems are powered, those connected directly to the battery.
- 'Idle': The engine is at idle mode, approximately with 750 revolutions per minute. All electronic systems are powered.
- '2000 rpm': The engine is running with 2000 revolutions per minute, and the gear is in neutral position. All electronic systems are powered.

During the measurements, no electronic system is turned on.

D. Transfer Function and Input Impedance

Using the measured S-parameters the channel frequency responses (H(f)) can be calculated. As described in [2], H(f) is function of both source and load impedances. However, if both impedances are equal to 50 Ω (Z_0), the channel transfer

function can be expressed as

$$H = \frac{S_{21}}{1 + S_{11}} \quad (1)$$

In [1][2] it is used $H = S_{21}/2$. The only difference is where the input reference plane voltage is located, including or not the source impedance. In our case the input reference plane is placed just at the input of the access points including the coaxial wires inserted with appropriate connectors to measure. The input impedance is calculated as

$$Z_{in} = Z_0 \cdot \frac{1 + S_{11}}{1 - S_{11}} \quad (2)$$

III. Measurements

A. Channel frequency response

A set of measurements has been carried out using as access points the described ones in section II-A. A connection is referred to as direct if the shortest path between the two access points does not pass through the battery, and as indirect in all other cases. The radio power supply and the cigarette lighter power supply are connected to the same fuse so the link established between them can be catalogued as direct. This link constitutes the only measured channel of this type. The measurements have been done the same day and consecutively to compare the three evaluated states.

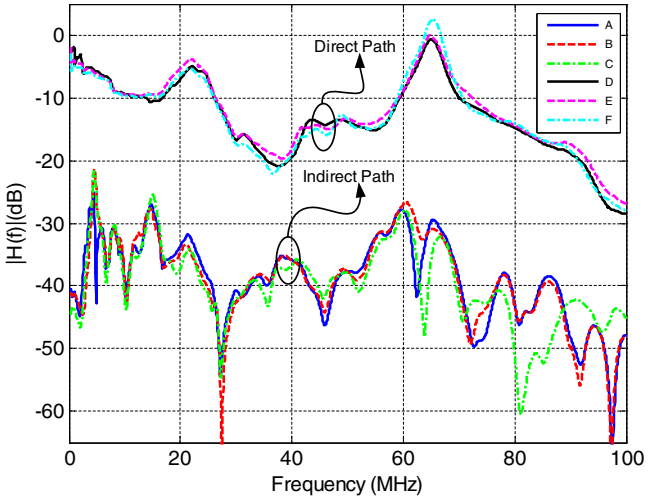

Fig. 4. Measured channel frequency responses for two different links: RearRBAC-FUSB (A) Off, (B) Idle, (C) 2000 rpm ; RADP-CIG (D) Off, (E) Idle, (F) 2000 rpm.

Fig. 4 draws the amplitude of the channel frequency responses of one direct and one indirect link, when the engine is turned off, is running and idle (750 rpm), and is running at 2000 rpm. As addressed in [1], the direct path presents a lower attenuation than the indirect path, and does not include deep frequency fading. The distance is not the essential factor for attenuation, but the pass or not through the battery. It is possible to find shorter paths with higher attenuation than longer ones. The higher frequency selectivity of the indirect channel is due to the multiple reflections that appear because of mismatching branches across the link between the access points. In indirect channels it is possible to find fading up to 25 dB. These effects are equivalents to the experimented ones on in-home power line channels [6]. Regarding the channel frequency response dependency on the engine speed, differences about 2 dB can be observed in magnitude of the direct channel frequency responses for the three engine states -off, idle, 2000 rpm- and of up to 15 dB in the indirect ones.

B. Noise

The noise has been recorded during 20 ms on the different access points for the three engine states considered. The Power Spectral Density (PSD) has been estimated by means of averaged periodogram method using a Hanning window of 20000 samples, which leads to a frequency resolution of 10 kHz. This resolution is more than enough to appreciate the presence of narrowband components (caused by periodic impulsive noise or interferences). In all the measurements, the noise PSD have a wide dynamic range of up about 60 dB. In Fig. 5 two noise PSD, measured at BAT and CIG points, and that can be considered as representative of the whole set are drawn. These noises have been selected by the proximity to the engine. As can be seen the background noise floor is between -115 dBm/kHz and -120 dBm/kHz. It must be highlighted the effect of FM radio on the noise measurements in the band 87.5 MHz-100 MHz, where narrowband components of high level over the background noise appear.

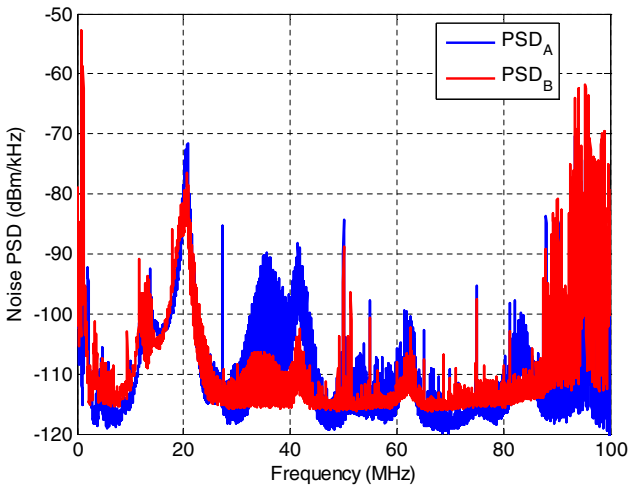

Fig. 5. Measured noise PSD at two different access points, PSD_A at the battery and PSD_B at the cigarette lighter.

C. Input impedance

The input impedance presents a large variation within the studied bandwidth from negligible values up to 1 kΩ (Fig. 6). The shape of the curves remembers a parallel resonant circuit. Both the number of resonances and the resonance frequency change according to the selected channel. However, these two parameters remain the same for the three measured engine states in a channel.

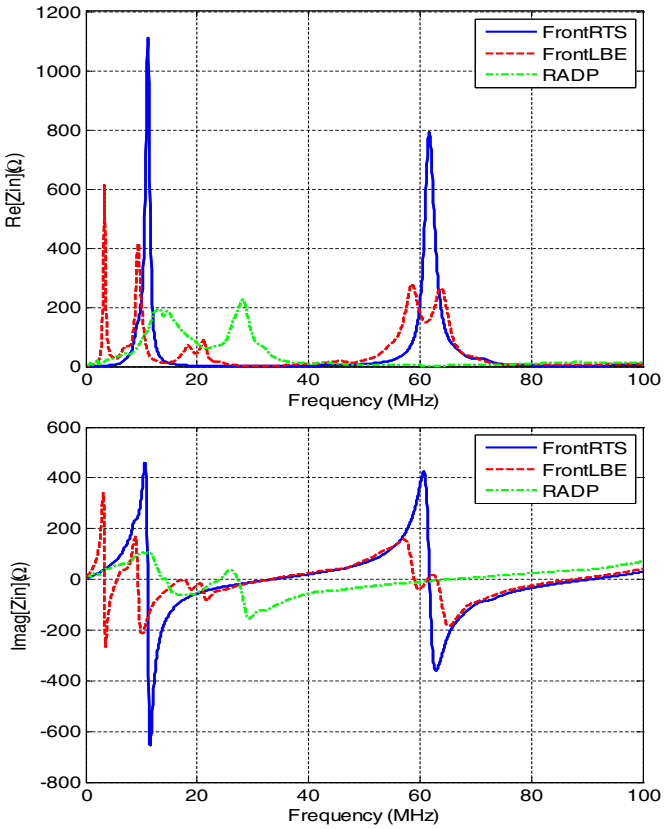

Fig. 6. Input impedance at the state 'Off'. Top: Real part. Bottom: Imaginary part.

IV. Statistical Analysis Of The Channels

In order to obtain a statistical characterization of the measured channels, the cumulative distribution functions (CDF) of the effective length of the impulse response (Fig. 7), the coherence bandwidth (Fig. 8) and the mean amplitude response (Fig. 9) have been computed. Representative values of these parameters and of the delay spread (mean and standard deviation) have been also calculated (Table I).

The delay spread (DS) is calculated according to

$$DS = T_S \sqrt{\frac{\sum_{n=0}^{L-1}(n-DM)^2|h[n]|^2}{\sum_{n=0}^{L-1}|h[n]|^2}} \quad (3)$$

where h[n] is the channel impulse response with length L and sampling period T_S, and DM is the mean excess delay defined as

$$DM = \frac{\sum_{n=0}^{L-1} n|h[n]|^2}{\sum_{n=0}^{L-1}|h[n]|^2} \quad (4)$$

The effective length (EL) is defined as the length of the shortest part of the channel impulse response whose energy is over a given percentage of the overall energy. In this paper, the percentage is set to 90%.

The coherence bandwidth (B_C) is defined as the frequency separation for which the spaced-frequency correlation function, given by

$$R(\Delta f) = \int_{-\infty}^{\infty} H(f)H^*(f+\Delta f)df \quad (5)$$

falls down a given threshold. In this work a 0.9 value has been used.

As the channel is frequency selective, the mean amplitude response is calculated according to

$$\bar{H}(dB) = \frac{1}{N}\sum_{k=1}^{N} 20log_{10}|H(k)| \quad (6)$$

where H(k) is the channel frequency response and N the number of frequency points.

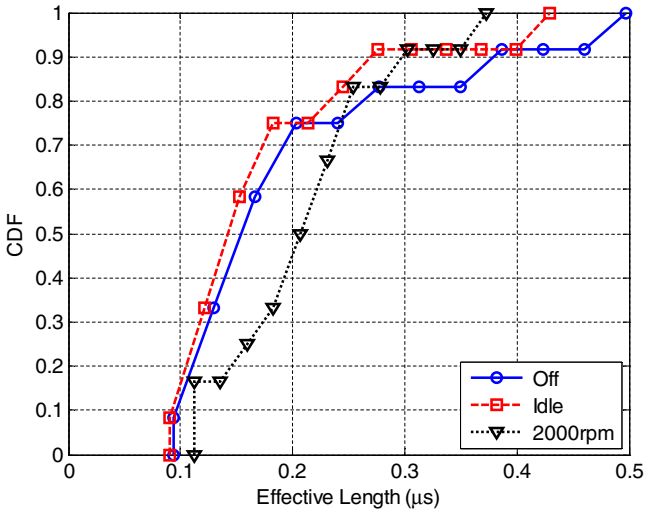

Fig. 7. CDF of the effective length

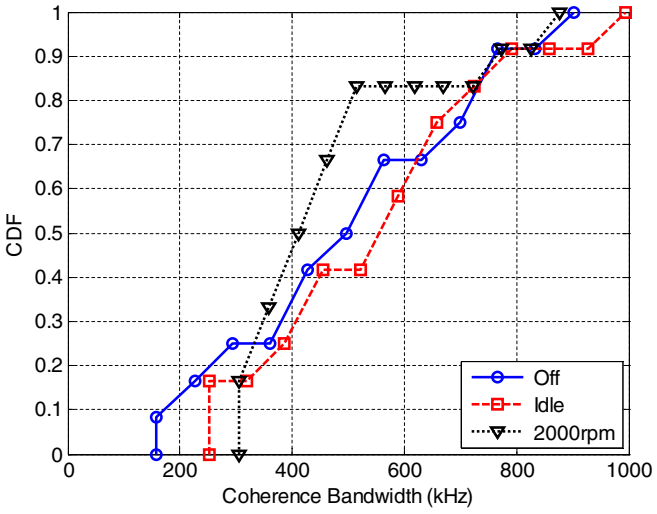

Fig. 8. CDF of the coherence bandwidth

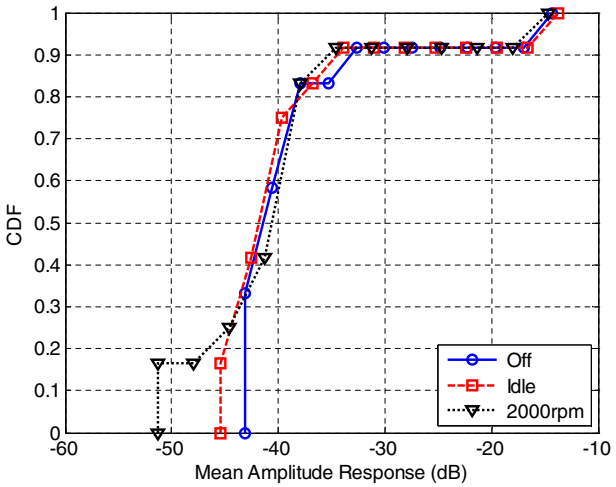

Fig. 9. CDF of the mean amplitude response

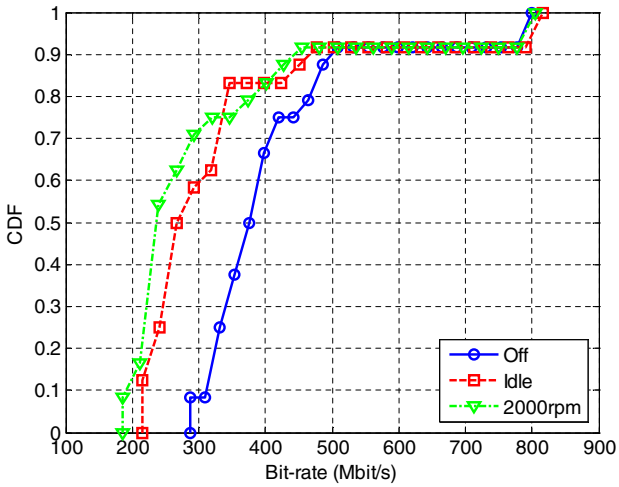

Fig. 10. CDF of the achievable bit-rate in the frequency band from 0 to 100 MHz based on the G.hn standard

TABLE I
STATISTICAL CHARACTERIZATION OF THE CHANNELS

	Off	**Idle**	**2000rpm**
DS mean (μs)	0.12	0.12	0.13
DS standard deviation (μs)	0.06	0.09	0.07
EL mean (μs)	0.21	0.18	0.22
EL standard deviation (μs)	0.13	0.1	0.08
B_C mean (kHz)	527.06	568.6	482.92
B_C standard deviation (kHz)	235.58	233.58	183.84
$\bar{H}$ mean (dB)	-37.93	-38.21	-39.15
$\bar{H}$ standard deviation (dB)	8.38	8.79	9.94

V. CHANNEL PERFORMANCE EVALUATION

In this section, the performance of an OFDM system based on G.hn standard is evaluated. Simulations have been accomplished using Binary PSK and square QAM constellations with a maximum of 12 bits per symbol and a BER constraint of 10^{-3}. The number of subcarriers is 4096, and an additional extension of 1024 samples is incorporated to each OFDM symbol, 512 samples to conform the guard interval and another 512 samples that result from the shaping of the OFDM signal. We set the transmitted power to -20 dBm/kHz in the band 2-30 MHz and to -50 dBm/kHz in the band 30-100 MHz. More information according to this standard and the way on which the OFDM symbol is constructed can be found in [5], [7]. In this work, a raised-cosine window is employed.

In the simulations, we have used the channel responses measured, 12 for each engine state, and the two noise PSD drawn in Fig. 5. Fig. 10 represents the achievable bit rate when the engine is off, idle and at 2000 rpm. There are remarkable differences between the three curves, which verify the influence of the engine speed on the system performance.

VI. CONCLUSION

In this paper, the application of PLC technology to the power grid of an automobile is discussed. For this purpose, some measurements have been carried out different links in a car to estimate both the channel frequency response and the received noise PSD. In particular, the influence of the engine state on the channel behavior has been studied. Afterwards, a statistical analysis of some behavioral parameters of the measured channels, to evaluate the time dispersion or frequency selectivity, is included. Finally, the achievable bit-rate obtained by simulating a multicarrier modulation system over these channels is presented.

ACKNOWLEDGMENT

This work has been supported by the Junta de Andalucía under project n^o TIC-03007. The authors would like to thank to Fiat Málaga for their collaboration.

REFERENCES

[1] M. Lienard, M. Carrion, V. Degardin, and P. Degauque, "Modeling and analysis of in-vehicle power line communication channels," *Vehicular Technology, IEEE Transactions on*, vol. 57, no. 2, pp. 670 –679, march 2008.

[2] M. Mohammadi, L. Lampe, M. Lok, S. Mirabbasi, M. Mirvakili, R. Rosales, and P. van Veen, "Measurement study and transmission for in-vehicle power line communication," in *Power Line Communications and Its Applications, 2009. ISPLC 2009. IEEE International Symposium on*, april 2009, pp. 73–78.

[3] V. Degardin, M. Lienard, P. Degauque, and P. Laly, "Performances of the HomePlug PHY layer in the context of in-vehicle powerline communications," in *Power Line Communications and Its Applications, 2007. ISPLC '07. IEEE International Symposium on*, march 2007, pp. 93 –97.

[4] P. Tanguy, F. Nouvel, and P. Maziearo, "Power line communication standards for in-vehicule networks," in *Intelligent Transport Systems Telecommunications,(ITST),2009 9th International Conference on*, october 2009.

[5] J. J. Sánchez-Martínez, J. A. Cortés, L. Díez, F. Cañete, and L. M. Torres, "Performance analysis of OFDM modulation on indoor PLC channels in the frequency band up to 210 mhz," in *Proceedings of the IEEE International Symposium on Power Line Communications and its Applications (ISPLC)*, March 2010, pp. 38–43.

[6] F. J. Cañete, L. Díez, J. A. Cortés, and J. T. Entrambasaguas, "Broadband modelling of indoor power-line channels," *IEEE Transactions on Consumer Electronics*, pp. 175–183, Feb 2002.

[7] V. Oksman and S. Galli, "G.hn: The new ITU-T home networking standard," *IEEE Communications Magazine*, vol. 47, pp. 138–145, October 2009.